Effect of flash butt welding parameters on mechanical properties of wheel rims

Efecto de los parámetros de la soldadura a tope por destello sobre las propiedades mecánicas de rines metálicos

Rodolfo Rodríguez Baracaldo, Mauricio Camargo Santos, Miguel Arturo Acosta Echeverría
Ingeniería mecánica, Universidad Nacional de Colombia, Sede Bogotá., Bogotá,Colombia.
Correo-e: rodriguezba@unal.edu.co

Resumen— Se estudian los efectos de las variables de proceso sobre la calidad de la soldadura a tope con destello en el acero SPFH 590. Las zonas metálicas soldadas y las zonas afectadas por el calor resultantes se analizaron mecánicamente utilizando pruebas de tracción, pruebas de flexión, pruebas de dureza Rockwell, y estructuralmente con microscopía óptica y microscopía electrónica de barrido. Los resultados indicaron una transformación de la junta metálica de ferrita laminar a la ferrita acicular. Durante el proceso de soldadura, los granos de forma alargada se tornaron a forma redondeada, y a través del proceso de enfriamiento, se formó una estructura de ferrita Widmanstatten. Se analizó la importancia de los niveles de los factores del proceso en la microestructura, la resistencia de la zona de soldadura y las características de la fractura. Los parámetros del proceso de soldadura, 5V (voltaje), 2.3 mm (upset) y 2 s (tiempo de destello), muestran la mejor combinación de propiedades (resistencia y ductilidad) para todas las pruebas realizadas.

Palabras clave— Flash Butt Welding, acero SPFH 590, voltaje, tiempo destello.

Abstract— The effects of process variables on weld quality are being studied for the Flash Butt Welding of SPFH 590 steel. The resulting welded metal and heat affected zones were characterized by tensile testing, bending testing, Rockwell hardness testing and microstructural analyzed by optical microscopy, and scanning electron microscopy. The results indicated a transformation of the metal joint from ferrite laminar to acicular ferrite. During the welding process, the long-shaped grains grew and became rounded-shaped, and through the cooling process, some side plate Widmanstatten ferrite structure is formed. The significance of process factor levels on microstructure, weld zone strength, and fracture characteristics were analyzed. The welding process parameters, 5V (voltage), 2.3 mm (upset), and 2 s (flashing time), displayed the best properties combination (strength and ductility) of all the test performed.
Key Word — Flash Butt Welding, SPFH 590 steel, voltage, flashing time.

I.   INTRODUCCIÓN

The Flash Butt Welding (FBW) process is a plane welding in which the opposing faces of the material are welded by one hit making it an extremely efficient process. In basic terms, it is a melting and a forging process capable of producing welded joints with strengths equal to those of the base materials [1-2]. This process makes part of the resistance welding processes with applications in welding plates, line pipes, rails, marine structures, vessel mooring chains and, particularly, in steel wheel rims in the automotive industry. [3].

The feature of FBW is directly influenced by the welding process parameters. It is essential to control multiple process variables to achieve the necessary joint requirements. Theoretical and experimental studies of the effect of FBW parameters have been reported in the literature. Most of them study welding process parameters such as changes in flashing time, upset time, upset current, flashing pattern, and upset dimension to maximize of tensile strength or fracture toughness and/or minimization of distortion, residual stresses, and porosity. [4-10].

The first outstanding work by Ziemian et al. studied the effect of some process variables. Sensitivity of the welding parameters on defects and inner inclusions could be observed through their statistical study [11]. Min and Kang studied the flash weldability of cold-rolling sheet and carbon steel used for the car bodies of automobiles; they determined that the resulting FBW was superior to laser [12]. Ichiyama et al. considered the effect on the fracture resilience that applies the FBW factors when it is used in high strength steels. There, it is concluded that the upset factor is the one to be controlled to improve the microstructure behavior and to decrease the inclusions in the welded zone [1]. Thus, a necessity of studying this type of welding in High Strength Low Alloying Steels (HSLA), with applications in the automotive industry is established.

The manufacturing of wheel rims in the automotive industry presents two requirements that must be satisfied for the use of

HSLA steels. The first one refers to the obligation of manufacturers of steel wheels of keeping and increasing the market participation of HSLA. The second one consists in working together with the automobile manufacturers in preserving the environment and developing fuel efficient automobiles. In the industrial production process of wheels, the rims are subjected to a series of processes such as bending, curling, and drawing which produces cracks in or near the weld zone sometimes due to the poor toughness of FBW joints which affects the safety and quality of the product. Therefore, the adequate combination of processing parameters of an AC welding machine for the FBW process will allow to weld HSLA steel sheets with the mechanical strength and welding discontinuities satisfying the requirements of steel wheel rims manufacturing. However, research regarding the strength of FBW joints in HSLA steel is relatively limited. The present work investigates the effect that the process variables (voltage, upset height, and flashing time) produce on the mechanical strength and the welding discontinuities of the FBW process. Some considerations are mentioned which could solve the user's difficulties in the application of this process and in the resulting quality of the products.

II. METHODS AND MATERIALS

The material used in this investigation correspond to SPFH 590 Japanese standard JIS G 3134 steel with thickness of 2.3mm [13]. The size of the specimens is 200 x 1086 mm. Table 1 registers the chemical composition.

Element	C	Si	Mn	P	Al	Fe
% Wt	0,09	0,13	1,69	0,013	0,031	bal

Table 1. Chemical composition of SPFH 590 JIS G 3134 steel [13].

The equipment for the welding procedure was a Swift-Ohio welding machine 91-AA model with a 400kVA capacity. The welding procedure is considered a two-stage electric resistance welding machine that produces the welded union in the whole area of both initially separated surfaces simultaneously. The first stage is the flash generation where heat is generated by the resistance against the electric current flow between the two surfaces to be welded. The second stage is called upset, which occurs when the separated surfaces, once at melting temperature, join abruptly through an axial force with a controlled speed [2,8]. Figure 1 shows a schematic of the process.

A similar process of the FBW exists, called upset welding; its use has been increasing in the manufacturing of automobile wheels rims. However, FBW is also frequently used in this industry [12]. The benefits of FBW are high speed, high efficiency, no pretreatment of the base material, high resistance in the welded joints and, finally, wide range of materials in which it can be applied [4,14].
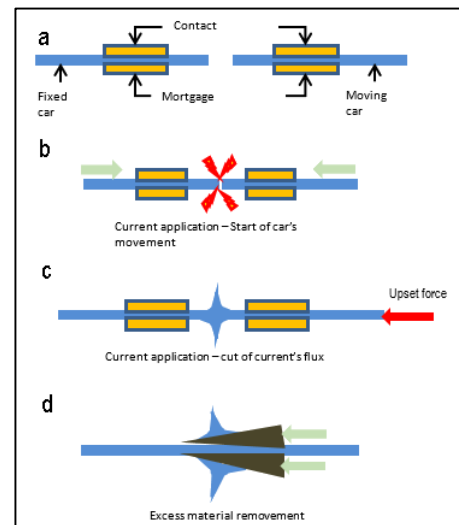

Figure 1. Schematic of the flash butt welding process.

The initial step of the process is to hold the pieces to be joined. At that point, the faces of the pieces to be welded start approaching. Once the flashing process has been completed, the mobile car accelerates quickly through the application of an axial force of considerable magnitude generating an intimate contact among the surfaces to be welded. This part of the process is called upset. Once the upset is over, the welded piece is removed. The expelled solidified material of the welded interphase is removed through a scraper machine.

Test specimens for 8 combinations were made with the following process parameters: Voltage, upset height, and flashing time. For each one of these parameters, two levels were defined: High and low. Special caution was taken in the random tests to eliminate preconditions that can skew the results. The values used in the process variables are shown in table 2. In table 3, the combination of the variables to create the treatments done on the welding is observed.

The manufactured specimens according to the AWS B4.0M: 2000 Standard [15] were used for the appearance evaluation; this evaluation also included the use of a magnifying glass and an optical stereoscope with the purpose of improving the defects detection over the heat affected zone (HAZ).

Designation	Welding Parameters	Low level		High level	
A	Voltage (V)	5	LV	7	HV
B	Upset height mm (calzo – mm)	2,3 (5,0)	LUH	4,6 (10,0)	HUH
C	Flashing time - seconds (car frequency- Hz)	2 (48)	LFT	4 (30)	HFT

Table 2. Welding parameters and factors levels.

Scientia et Technica Año XXII, Vol. 23, No. 01, marzo de 2018. Universidad Tecnológica de Pereira.

53

After manufacturing the specimens, visual inspection was done over an area with day-light fixture along with a 10X magnifying glass. The microstructure was evaluated with a Leco 100x – 800x software IA32 optical microscope and a FEI Quanta model 200 Scanning electron microscope (SEM), which was also used to perform the fractographic analysis. The Knoop microhardness was done with a Leco model LM 100AT equipment. The specimens fabricated for the microstructure and microhardness were taken from HAZ. Grinding, polishing, and chemical etching with 5% Nital were done to reveal the microstructure.

Treatment	Variables combination
1	LV, LUH, LFT
2	LV, LUH, HFT
3	LV, HUH, HFT
4	LV, HUH, LFT
5	HV, HUH, HFT
6	HV, HUH, LFT
7	HV, LUH, HFT
8	HV, LUH, LFT

Table 3. Specimen numbers and associated treatment combinations (L: low, H: high).

The bending tests were done with a 60-ton hydraulic press. The specimens (38 X 150 X 3 mm) were mounted on a device designed and fabricated in this investigation following the AWS B4.0: 2000 Standard recommendations. The test speed was 1m/min at room temperature according to the established parameters in the referenced standard [15]. The specimens for the tensile test of the welded joint were elaborated according to the Japanese JIS G 3134 Standard [13]. A schematic of each one of the specimens can be observed in Figure 2.
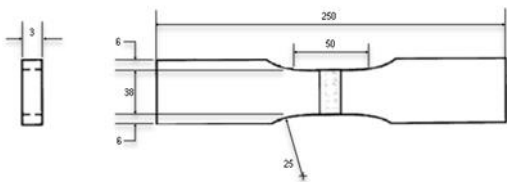

Figure 2. Tensile resistance specimen. Adapted from [13].

III. RESULTS AND DISCUSSION

A. Structural analysis.

Visual inspection was carried out with acceptable results in every specimen. This inspection reported a symmetrical surface appearance of the joint and the HAZ; cracks or superficial defects were not found on the surface. This suggests that the combinations of the three different parameters to weld the specimens offered a satisfactory superficial appearance even at the combination of low voltage and high upset.

Figure 3 presents the obtained images from optical microscopy over the base material and the welded zone. Figure 3 shows the initial condition of material, a long-shaped laminar ferritic structure due to the hot rolling process. The structure of this HSLA steel corresponds to ferritic-pearlitic in which the properties are determined by its dominant structure, the ferrite. Figure 4 shows the SEM images of the base material with pearlite structure (light highlighted gray) and ferrite (dark gray at bottom).
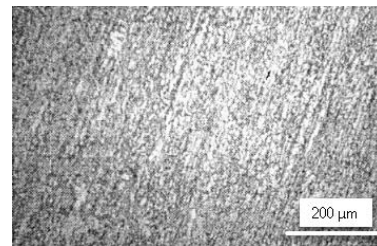

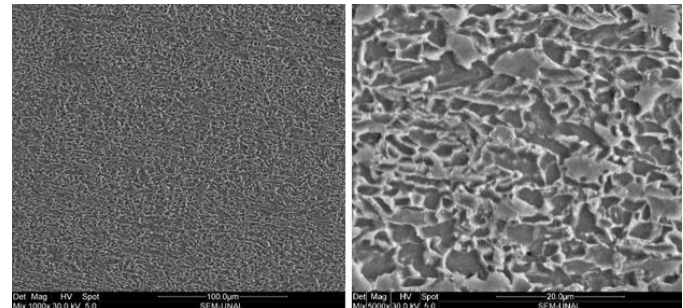Figure 3. Optical Micrographs of image base material sheet (SPFH 590).

Figure 4. SEM Micrographs of the base material.

Figure 5 shows the optical micrographic images of acicular ferrite (light color) of the welded joint. It is observed that the ferrite changes from laminar shape (which is present in the base material) to acicular ferrite. Throughout welding process, the long-sized grains become round-shaped. During the cooling process, Widmanstatten Ferrite structures are formed according to the Dubé's classification system. The phase is also referred to in the study made by Zieman et al. [11].
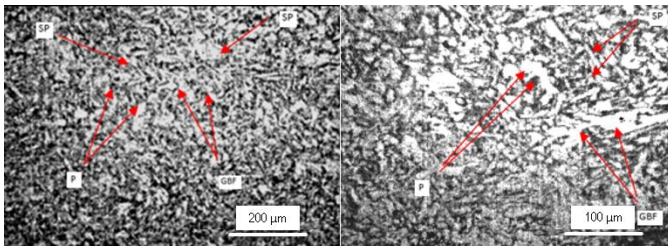
Figure 5. Optical Micrographs of Acicular Ferrite (light color) of the (upset joint) welded joint. GBF: Grain boundary Ferrite. WSP: Widmanstatten side-plate Ferrite. P: Pearlite.

The acicular ferrite may increase or retain the ultimate tensile strength to the same level of base material. However, the generation of Widmanstatten Side-Plate Ferrite could generate a brittle welding increasing the risk of premature fractures, as was pointed out by Kumar et al. [16].

Figure 6 shows SEM images of the welded zone and the base material. Figure 6a) corresponds to the HAZ, that shows, just like the optical micrographic images, the same distribution of acicular ferrite. And Figure 6b) corresponds to the base material. In the research by Ricks et al. it is established that acicular ferrite is the result of an intergranularly nucleation of Widmanstatten ferrite in HSLA steels [17] which can be placed in the same level of this study due to the use of the same steel and the similarities in the welding process.
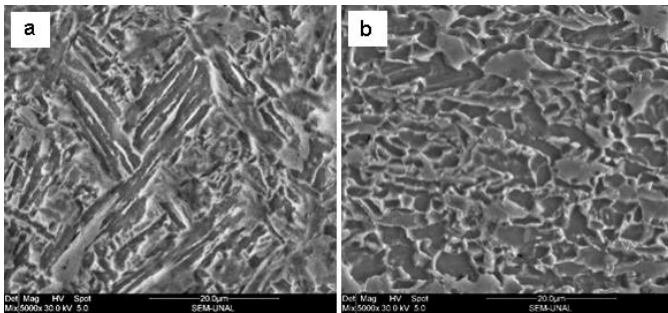

Figure 6. SEM Micrographs. a) Joint zone, b) Base material

Figure 7 shows optical microscopic images of the transversal section of the welded joint. It is observed a white vertical line which refers to decarburized layer due to the carbon of base metal diffusing into the welded area during flashing process which is expelled in the upsetting process. Decarburization is characteristic on this type of resistance welding. Kim et al., also reported these kinds of discontinuities in their work about effect of FBW parameters on the mechanical properties of steel mooring chains for offshore structures [9].

Figure 7. Optical Micrographs of macro section of Flash Butt Welding. White line indicates the decarburized zone.

B.   Mechanical characterization.

Table 4 summarizes the results of the behavior of the ultimate tensile strength (UTS) and strain (% Elong) for every specimen. The presence of fracture in the welding joint of the specimens of treatments 3 and 8 shows that these welds are not adequate since failure occurs outside the zone where the joint was done. Similarly, Centinkaya et al., reported failure in the HAZ demonstrating that this zone has lower strength due to the thermal effect and, therefore, it is also rejected [18]. Tensile strength decreases in function of the increase of power required for the welding. The rise of energy given to the material generates a grain growth in the HAZ, which causes a strength loss in the joint, as it was observed by Sharifitabar et al. [19]. On the other hand, a greater heat input produces a considerable amount of Widmanstaten phase. The shape of the plates of this phase increases the stress concentration in this region and, thus, decreases the joint strength.

Table 4 shows that specimens with tensile strength value beneath 590 MPa are the ones that had fracture in the welding zone (Specimens with treatments 2, 3, and 8). According with base material properties [13], the ductility must be higher than 22%. The specimens with treatments that surpass this value are 1, 4, 6 and 7. Consequently, the welding parameters to obtain specimens with treatment 1 and 7 are the ones which present a good behavior meeting the strength and ductility requirements. Specimens with treatment 2, 3 and 8 show elongation percentage values lower than the 5% and these same specimens fractured in the welded zone which tells that they present a brittle behavior caused by a greater input heat that produces a considerable amount of Widmanstaten phase. The shape of the plates of this phase increases the stress concentration in this region producing poor elongation.

Treatment	UTS (MPa)	Elong. (%)
Base	624	22
1	596.85	30

2*	392	2.5
3*	546	10.65
4	599.85	24.55
5	578.35	19.95
6	575.1	22
7	590.4	27.75
8*	369.6	2.1

Table 4. Average results ultimate tensile test (*Joint fails).

Figure 8 shows the specimens with treatment 1 and 7 already tested. These are the ones which presented better and outstanding ductility and tensile strength values. The welding parameters with the defined operating conditions, such as low-level voltage (LV), low upset height level (LUH), and low flashing time level (LFT), can be seen in table 3. Those specimens showed suitable properties because of the welding process parameters which allow for the ring manufacturing.
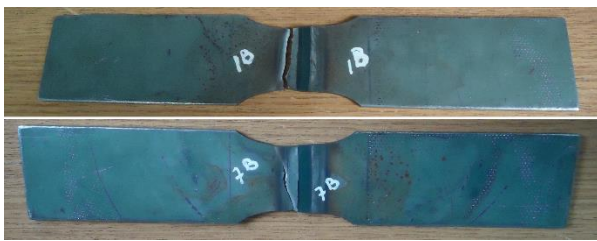

Figure 8. Tensile test specimens which presented a fracture outside the welded join; a) with treatment 1 and b) with treatment 7.

Figure 9 shows the Knoop micro-hardness test results performed over the HAZ. The average values for each treatment are presented. The negative values correspond to the points that were taken at the left side and positive values taken at the right side from the central joint zone; each one of these points are separated 0.5 mm which makes a total distance of 3.5 mm to the right and 3.5 mm to the left from the center. The hardness values, greater towards the joint zone, can be ascribed to: 1) the base microstructure becomes Widmanstatten Ferrite structure, and 2) the hardening due to deformation caused in the generation of the upset in the welding process. The majority of the specimens displayed similar hardness profiles with the maximum hardness within the weld zone and decreasing hardness at the HAZ zone up to the base metal.
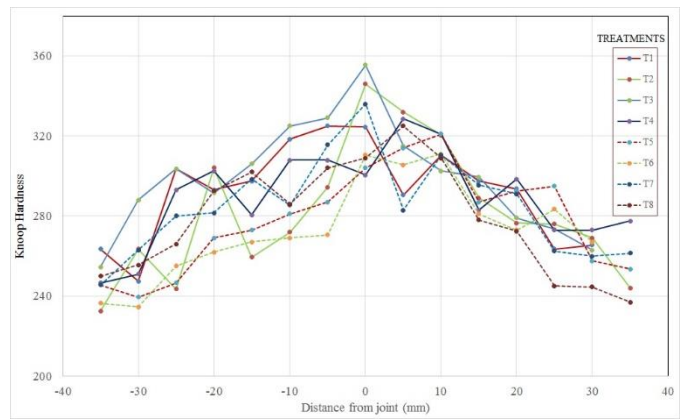

Figure 9. Knoop microhardness of the specimens for each treatment.

The results of the bending test showed that treatments 2, 5, and 8 do not meet the test requirements presenting a total fracture in the welded joint. As mentioned before, treatments 2 and 8 also presented low ductility in tensile test. The remaining specimens comply with the requirements of the test satisfactorily. Figure 10 displays some images of the results of the bending test. Figure 10b shows the specimen with treatment 1 meeting the requirements of the test. On the contrary, Figure 10c shows that specimen 2 does not meet the requirements.
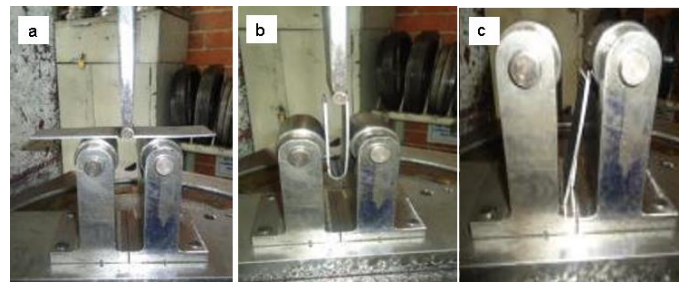

Figure 10. Bending test imagines. a) Experimental arrangement; b) Specimen 1 meeting the requirements of the test; c) Specimen 2 does not meet the requirements.

A brittle behavior is observed in the welded specimens in which heat entrance conditions were greater. According with the experimental design exposed in table 2, the specimens with treatments 2 and 5 received more heat during the welding process because of a high time flashing level. Additionally, the specimens with treatments 5 and 8 received more heat because of a high voltage level which generated more heat during the welding process. This result agrees with the work by Singh, et al. where it was observed that the welded specimens with low heat entrance have a higher ductility than those manufactured with a high heat entrance [20].

C. Fractographic analysis.

Figure 11 shows SEM micrograph of fracture surface of the specimens with treatment 4, which displays a fracture outside the welding joint. As it is seen in Figure 11 a), this is a ductile

fracture characterized by the presence of micro voids. This type of fracture is caused by the coalescence of microfisures that nucleate in regions where discontinuities exist and are associated with second phase particles, inclusions, grain boundaries, and dislocations. As strain increases, the microfisures grow and eventually form a continuous fracture. Similarly, if the inclusions where voids nucleate are long, as it happens with rolled steels, the ductility measured perpendicularly to the rolling direction is poor which generates a laminar tear, as shown in Figure 11 b).
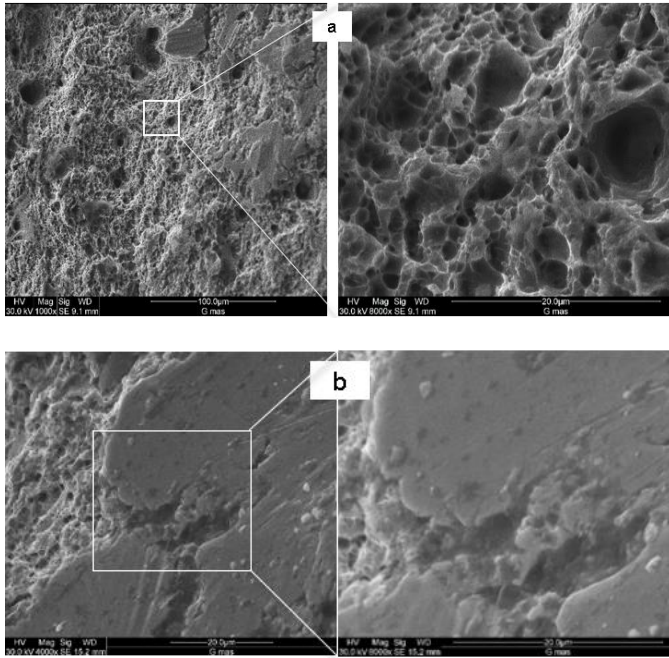

Figure 11. SEM micrograph of fracture surface of the specimen with treatment 4. a) Ductile fracture outside the welding joint; b) Poor ductility perpendicular to the rolling direction.

Figure 12 shows SEM micrograph of the fracture surface on welding joint of the specimens with treatment 8. In Figure 12 a), a mixed fracture composed by cleavage fracture that propagates throughout the grains (transgranular) and the propagation of the fracture around the grain boundaries (intragranular) showing micro-dimple zones belonging to ductile fracture zones is distinguished. Figure 12 b) shows superficial cracking caused, possibly, by the hydrogen that settles beneath the welding or inside it. This hydrogen, diffused from the welding zone to the HAZ zone, accumulates in the discontinuities that occur beneath the grains (underbead cracks). Simultaneously, the hydrogen pressurizes as gas generating a high internal stress perpendicular to the plane face of the accumulation. This phenomenon is relatively frequent in welding performed in high strength structural steels (with a yielding strength up to 500 MPa) [21].
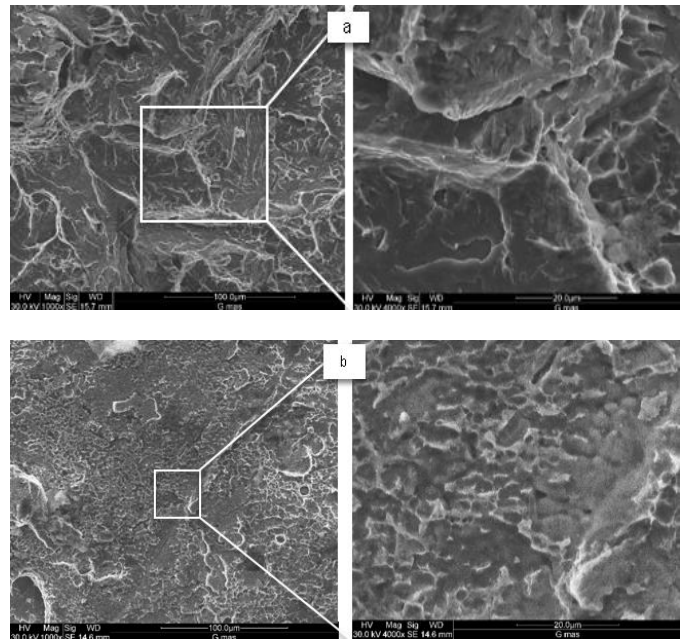

Figure 12 a) SEM micrograph of the fracture surface on welding joint of the specimen of treatment 8. b) Superficial cracking.

IV.   CONCLUSIONS

The microstructure and mechanical properties results of eight parameters settings of the FBW process performed over the SPFH 590 steel were evaluated adequately using tensile testing, bending testing, Rockwell hardness testing, optical microscopy, and scanning electron microscopy.

The microstructural analysis of the joint shows the transformation from ferrite laminar to acicular ferrite. During the welding process, the long-shaped grains grow and become rounded-shaped; moreover, during the cooling process some side plate Widmanstatten ferrite structure forms. The mechanical behavior was evaluated through hardness tests, tensile test, and bending tests. The results showed a different behavior for the several combinations of parameters performed.

Welding process parameters, 5V (voltage), 2.3 mm (upset), and 2 s (flashing time), displayed the best properties combination (strength and ductility) of all the test performed. These results apply to reduce the rejected parts in the manufacturing processes of structural elements produce by the FBW.

REFERENCES

[1]. Y. Ichiyama, and K. Shinji, "Flash-Butt Welding of High Strength Steels," Nippon Steel Technical Report Vol. 95, Jan. 2007 .

[2]. Flash Welding chapter in ASM Handbook: Welding, Brazing, and Soldering, Vol.6, 10th, Ed., by K. Ferjutz, J. Davis, Ed. ASM International, United States, 1994.

[3]. AWS Welding Handbook: Welding Processes, Vol. 2, 8th Ed., by R. L. O'Brien, American Welding Society/Welding Handbook, United States,

[4]. D. E. Ziemian, C. W. Sharma, and M. M. Whaley, "Flash butt-welding process optimization through the design of experiments" presented at Proc of Int Conf. on NSF Engineering Research and Innovation Conference, Knoxville, Tennessee USA, 2008.

[5]. F. Zhang, B. Lv, B. Hu, and Y. Li, "Flash butt welding of high manganese steel crossing and carbon steel rail", Mater Sci Eng A, Vol. 454–455, pp 288–292, Apr. 2007.

[6]. D. Tawfik, P. Mutton, and W. Chiu, "Experimental and numerical investigations: Alleviating tensile residual stresses in flash-butt welds by localized rapid postweld heat treatment", J Mater Process Technol, Vol. 196, pp 279–291, Jan. 2008.

[7]. C. Barbosa, J. Dille, J. L. Delplancke, J.M.A Rebello, and O. Acselrad, "A microstructural study of flash welded and aged 6061 and 6013 aluminum alloys," Mater Characterization, Vol. 57, pp 187-192, 2006.

[8]. N.F.H. Kerstens, and I.M. Richardson, "Heat distribution in resistance upset butt welding" J Mater Process Technol, Vol. 209, pp 2715–2722, Aug. 2009.

[9]. D. Kim, Q. So, and M. Kang, "Effect of flash butt welding parameters on weld quality of mooring chain", Arch Mater Sci Eng A, Vol. 38(2), pp 112–117, 2009.

[10]. M. Sharifitabar, and A. Halvaee, "Resistance upset butt welding of austenitic to martensitic stainless steels", Mater Des, Vol. 31, pp 3044–3050, 2010.

[11]. C. W. Ziemian, M. M. Sharma, D. E. Whaley, "Effects of flashing and upset sequences on microstructure, hardness, and tensile properties of welded structural steel joints", Mater Des, Vol 33, pp 175-184, 2012.

[12]. K.B. Min, K.S. Kim, and S.S Kang, "A study on resistance welding in steel sheets using a tailor-welded blank (1st report) Evaluation of upset weldability and formability", J Mater Process Technol, Vol. 101, No. 1–3, 14, pp 186-192, Jan. 2000.

[13]. JIS HANDBOOK, "JIS G 3134:2006. Hot-rolled high strength steel plate, sheet and strip with improved formability for automobile structural uses", Ferrous Materials & Metallurgy II, by JSA Japanese Standards Association, Tokyo Japan 2006.

[14]. N. Kerstens, Investigation and Control of Factors Influencing Resistance Upset Butt Welding, Delft.: Thesis Master dissertation. TU Delft, 2009.

[15]. AWS, "AWS B4.0M:2000," Standard Methods for Mechanical Testing of Welds, American Welding Society, 2000.

[16]. A. Seshu-Kumar, B. Ravi-Kumar, G.L. Datta, and V.R. Ranganath, "Effect of microstructure and grain size on the fracture toughness of a micro-alloyed steel," Mater Sci Eng A, Vol. 527, No. 4-5,15, pp 954-960 Feb. 2010.

[17]. R. Ricks, P. Howell, and G. S. Barritte, "The nature of acicular ferrite in HSLA steel weld metals," J. Mater. Sci. Vol. 17, pp 732–740, Mar. 1982.

[18]. C. Centinkaya, and U. Arabaci, "Flash butt welding application on 16MnCr5 chain steel and investigations of mechanical properties," Mater Des, Vol. 27, pp 1187-1195, Nov. 2006.

[19]. M. Sharifitabar, A. Halvaee, and S. Khorshahian, "Microstructure and mechanical properties of resistance upset butt welded 304 austenitic stainless steel joints," Mater Des, Vol. 32, pp 3854-3864, Aug. 2011.

[20]. T. Singh, A. Shahi, and M. Kaur, "Experimental studies on the effect of multipass welding on the mechanical properties of AISI 304 stainless steel SMAW joints", Int. J. Sci. Eng. Research, Vol. 4, pp 951-961, Dec. 2013.

[21]. H. Bang, H. Bang, C. Ro, and S. Jeong, "Mechanical Behavior of the Weld Joints of Thick Steel Plates Produced by Various Welding Processes", Strength Mater, Vol 47, pp 213–220, Jan. 2015.